FRAGMENTATION OF RELATIVISTIC NUCLEI

Bruce Cork
Lawrence Berkeley Laboratory
University of California
Berkeley, California 94720 U.S.A.

ABSTRACT

Nuclei with energies of several GeV/n interact with hadrons and produce fragments that encompass the fields of nuclear physics, meson physics, and particle physics. Experimental results are now available to explore problems in nuclear physics such as a) the validity of the shell model to explain the momentum distribution of fragments b) the contribution of giant dipole resonances to fragment production cross sections c) the effective coulomb barrier d) nuclear temperatures. A new approach to meson physics is possible by exploring the nucleon charge exchange process. Particle physics problems are explored by a) measuring the energy and target dependence of isotope production cross sections, thus determining if limiting fragmentation and target factorization are valid, b) measuring total cross sections to determine if the factorization relation,

$$\sigma_{AB}^2 = \sigma_{AA} \cdot \sigma_{BB} \text{ is violated}$$

Also, new experiments have been done to measure the angular distribution of fragments that could be explained as nuclear shock waves, and to explore for ultradense matter produced by very heavy ions incident on heavy atoms.

INTRODUCTION

Theories that describe large baryon number hadronic interactions have been very distinct from theories that describe small baryon number interactions. The result is that "nuclear" physics and "particle" physics are usually regarded as difference subjects. Chew[1,2] has pointed out that one reason for the difference in approach is that the energy level spacing for low baryon number, (e.g. B=0, 1) are orders of magnitude higher than for $B \geq 2$.

The interactions of relativistic heavy ions could be expected to have some of the properties of single hadron-hadron collisions. In particular, limiting fragmentation and factorization could be expected at energies of a few GeV/n. The interaction radius increases with projectile mass, thus the classical limit of the center of mass wavelength being much less than the interaction radius is easily satisfied. The center of mass momentum for a projectile M_p incident on a target M_T is

$$P \simeq (\gamma M_p M_T)^{\frac{1}{2}}/2$$

For example, a 2 GeV/n ^{12}C incident on ^{205}Pb has $P \simeq 60$ GeV/c and a center of mass wavelength.

$$\lambda = \frac{h}{p} \simeq 10^{-18} \text{ cm.}$$

which is much smaller than the interaction radius.

Relativistic heavy ions incident on nucleons or nuclei interact, producing fragments that can be described in terms of three different processes. If inclusive reactions of the type,

$$A+B \rightarrow C+G$$

are observed, where only particle C is detected and G is any allowed final state of the system, then it is convenient to introduce a new dynamic variable,

$$X = \frac{P_L^C(\text{C.M.})}{E(\text{C.M.})/2}$$

where P_L^C (C.M.) is the longitudinal center of mass energy of the particle C and E (C.M.) is the total center of mass energy. The allowed range of X is from -1 to +1, and for positive X in high energy reactions,

$$X \simeq \frac{E^C \text{ (Lab)}}{E_{TOT}\text{(Lab)}}$$

Thus X is the fraction of energy carried off (in the lab frame) by particle C. The three different processes of fragmentation are illustrated by Fig. 1. Consider two particles A+B colliding in their center of mass frame, the fragments with $X \simeq +1$ are fragments of the projectile, the fragments with $X \simeq -1$ are fragments of the target and fragments with $X \simeq 0$ are fragments which have been essentially at rest in the center of mass system, the central or pionization fragment region. These processes can also be described in terms of another variable, the rapidity $[Y=\tanh^{-1}(P_{\parallel}/E)]$. Projectile fragments typically have $Y \geq +1$, target fragments $Y \leq -1$, and pionization events $Y \simeq 0$. Events of these types in photographic emulsion are shown by Figs. 2,3. The relative fragmentation probabilities for 2.0 GeV/n ^{16}O incident on photographic emulsion are approximately 15% each for projectile and target fragmentation and 70% for central collisions.

Fortunately there is an extremely powerful experimental method of exploring the fragmentation process. For example, an inclusive experiment can be done with relativistic ^{12}C (projectile) + (target). All of the fragments of the projectile have high velocity in the lab and can be analyzed in a magnetic spectrometer. With the aid of momentum analysis, time of flight, and $\frac{dE}{dX}$, all of the fragments can be directly identified. Nature has even been very kind because longitudinal and transverse momenta of the fragments in the projectile frame of reference are small, thus the solid angle of the detector system can be quite small.

A brief summary of several experiments follows:

Isotope Production Cross Sections From Fragmentation of ^{16}O and ^{12}C at Relativistic Energies. P. J. Lindstrom, D. E. Greiner, H. H. Heckman, Bruce Cork, F. S. Bieser. LBL 3650

Measurements have been made of the production cross sections of fragments from 2.1 and 1.05 GeV/n ^{16}O and ^{12}C incident on targets of H, Be, C, Al, Cu, Al, and Pb. Table I of LBL 3650. The fragments are fragments of the projectile and not fragments of the target because they retained the momentum per nucleon, i.e. $\beta\gamma$ of the projectile. The nucleon-pick-up cross section was less than 10 μb, however, pion charge exchange was greater than 30 μb.

The cross sections σ_{BT}^{F} for production of a fragment F by a beam particle B on target T can be compared with the inverse reaction, protons on nuclei at high energies. For proton energies >600 MeV, 42 measured cross sections for 15 different secondaries have been compiled.[3,4] There is good agreement between these values and the measured values, Table I LBL 3650.

At high energies, target factorization is predicted for peripheral collisions. In this experiment it was observed that the cross sections can be factored,

$$\sigma_{BT}^{F} = \gamma_{B}^{F} \cdot \gamma_{T}$$

where γ_{BT}^{F} depends only on the projectile and fragment and γ_T is the target factor, Fig. 4. Exceptions to strict factorization are 1) γ_T for a hydrogen target has a weak dependence on the mass of the fragment A_F i.e. $\gamma_T(H) = 0.66 + 0.028\ A_F$. 2) For single nucleon stripping, γ_T is enhanced for high Z targets. This is in agreement with the calculated[5] contribution for Coulomb dissociation assuming a giant dipole resonance, in the target's virtual photon field. The coulomb dissociation part of the cross section has been computed[5] and subtracted from the measured σ_{BT}^{F}. The magnitude of this correction is given in Fig. 5. The resultant cross sections are consistent

with the target factor given in Table I LBL 3650. The target factors fit the data with a confidence level of 0.6 and are an approximate fit to either,

$$\gamma_T = A_T^{\frac{1}{3}} \text{ or } \gamma_T \simeq (A_B^{1/3} + A_T^{1/3} - 1.6)$$

In either case the interaction is interpreted to be a peripheral interaction with the target. However, neither formulation for γ_T explains the observed structure, in particular the results $\gamma_T(\text{Be}) > \gamma_T(\text{C})$. It is apparent that $\gamma_T(\text{He})$ should be measured.

A more accurate fit to the data is,

$$\gamma_T = kt^n(r_t + b)$$

where r_t is the measured half density electric-charge radius and t is the measured charge skin thickness of the target measured by electron scattering[6]. The three fitted variables are: the exponent n=0.5, b=3.0 fm., and normalizing constant k=0.26. This formula is consistent with the measured structrue in the mean target factor to an accuracy of better than 2%, and with a confidence level of 0.9. Since σ_{BT}^F factors, and the momentum distributions are target independent[7], the partial cross sections factor — a result expected by limiting fragmentation models. From the present data it cannot be determined whether γ_T contains projectile-dependent terms, e.g. the sum of the projectile and target nuclear radii.

The cross sections for isotope production were observed to be energy independent for 1.05 and 2.1 GeV/n ^{12}C. and agree with the production cross sections at 600 MeV.[3,4]. Also, except for charge exchange reactions, the ratio,

$$\frac{\sigma_{BT}^F(^{16}O)}{\sigma_{BT}^F(^{12}C)} = 0.4 \text{ to } 1.35$$

even though the individual cross sections vary over three orders of magnitude; Furthermore, 40% of the above ratios are in the interval 1.0 ±0.15.

The production ratios of fragments of mirror nuclei should give insight into the mechanism that produce final states. Evaporation models would preferentially evaporate neutrons resulting in $\sigma_N/\sigma_P \leq 1$ where σ_N/σ_P is the production cross section for mirror fragments neutron rich to proton rich, of the same projectile and target. Also, if a neutron skin extends beyond the proton surface,

a stripping process would also result in $\sigma_N/\sigma_P \leq 1$. It is observed that, to the contrary, $1.0 < \sigma_N/\sigma_P < 4.1$ with most values being in the interval 1.0 to 1.7. It is concluded that the binding energy of the final state fragment must influence this ratio. For example, the mass excess vs σ_{BT}^F for isobars shows the fragments with the lower mass excess have the higher production cross section. The projectile fragmentation cross section is thus interpreted as a peripheral fragmentation process.

An experiment of the inverse reaction is;

PRODUCTION CROSS SECTIONS OF Be ISOTOPES IN C AND O TARGETS BOMBARDED BY 2.8 GeV ALPHA PARTICLES: IMPLICATIONS FOR FACTORIZATION.

G. M. Raisbeck and F. Yiou
Laboratoire Rene Bernas du Centre de Spectrometrie Nucleaire et de Spectrometrie de Mass, 91406 ORSAY, France

ABSTRACT: The production cross sections of ^{7}Be in C and O, and ^{9}Be and ^{10}Be in C targets irradiated by 2.8 GeV alpha particles have been measured. The results are discussed in terms of the applicability of a factorization relationship proposed for high energy nuclear cross-sections.

PREPRINT - To be published.

In another experiment the momentum distributions of the fragments are given in the following:

MOMENTUM DISTRIBUTION OF ISOTOPES PRODUCED BY FRAGMENTATION OF RELATIVISTIC ^{12}C and ^{16}O PROJECTILES

D. E. Greiner, P. L. Lindstrom, H. H. Heckman, Bruce Cork, and F. S. Bieser
LBL 3651 To be Published

It has been observed that the momentum distributions in the projectile frame are typically Gaussian, narrow in angle and momentum spread, and isotropic. The distributions depend on projectile and fragment but correlation with the target mass or beam energy was not significant.

The experiment was done simultaneously with the previous cross section experiment using the single-focusing magnetic-spectrometer. Particle trajectories were measured with multiple-wire proportional chambers. The longitudinal and transverse momenta, $P_{\parallel}$ and $P_{\perp}$, were obtained from the rigidity and direction of the fragment at the focal plane of the spectrometer.

The longitudinal-momentum distribution, in the projectile rest frame exhibits a strikingly good fit to a Gaussian distribution,

Fig. 6. The fitted variables are amplitude, central momentum $< P_{\parallel} >$ and standard deviation $\sigma_{P_{\parallel}}$. For the various isotopes, $\sigma_{P_{\parallel}}$ varies over the range 50 to 200 MeV/c and the average momentum $< P_{\parallel} >$ is slightly negative relative to the projectile.

If there is a large separation in rapidity $[Y=\tanh^{-1}(P_{\parallel}/E)]$ between the target and fragment momentum distributions, then limiting fragmentation is valid if the shape of the momentum distribution is independent of target and projectile energy.[8] The target and energy dependence of $< P_{\parallel} >$ and $\sigma_{P_{\parallel}}$ were examined for all isotopes. There was no dependence on target mass above the 5% level for σ_{P} and above the 10% level for $<P_{\parallel}>$. Also for ^{12}C, $\sigma_{P_{\parallel}}$(2.1 GeV/n/$\sigma_{P_{\parallel}}$(1.05 GeV/n)= 1.02±0.02 and $< P_{\parallel} >$ (2.1 GeV/n)- $<P_{\parallel}>$ (1.05 GeV/n)=1.0±2.0 MeV/c. It is concluded that the limiting fragmentation region is reached before 1.05 GeV/n.

Since the momentum distribution of the fragments depends only on the identify of the projectile and fragment, it has been possible to parameterize the mass dependence by a simple function $\sigma^2_{P_{\parallel}}(B,F)= 4\sigma_o^2\, F(B-F)/B^2$, shown in Fig. 7, where B and F are the mass numbers of the beam and fragment nuclei, respectively. The fitted variable σ_o is listed in Table I. The parabolic shape displays the general trend of the data but the variations from the smooth curve are interpreted as evidence for nuclear structure effects. Evidence for this is enhanced by the observation that the same complex variation of $\sigma_{P_{\parallel}}$ with fragment mass is exhibited by both the ^{16}O and ^{12}C fragments.

The parabolic dependence of $\sigma^2_{P_{\parallel}}$ on fragment mass of the form

$$\sigma^2_{P_{\parallel}} \propto F(B-F)$$

was first predicted by Wenzel,[9] later by Lepore and Riddell[10], and indirectly by Feshbach and Huang[11] as extended by Goldhaber[12]. Lukyanov and Titov[13] have assumed the fragmentation process to proceed in two stages and obtain results in good agreement with experiment.

The parabolic shape arises when one assumes:

1) The fragment momentum distributions are essentially those in the projectile nucleus.
2) There are no correlations between the momenta of different nucleons and
3) Momentum is conserved.

The results of these theories are compared with experiment in Table I. The quantum mechanical model of Lepore and Riddell [10] is a calculation that employs the sudden approximation with shell model wave functions to predict,

$$\sigma_o^2 = \frac{1}{8} M_p B^{\frac{1}{3}} \left[45\, B^{\frac{1}{3}} - 25\right] \left(\frac{MeV}{C}\right)^2$$

This relation, where M_p is the proton mass, is in good agreement with the experimental values. Feshbach and Huang[11] assume sudden emission "Virtual Clusters" and relate σ_o to the Fermi momentum of the projectile, P_f. Using the formulation due to Goldhaber[12], the relation between P_f and σ_o is

$$\sigma_o^2 = \frac{1}{20} P_f^2 \, B^2/B-1$$

The elastic electron scattering experiments give higher values of P_f and predict values of σ_o that are 25% higher than the measured fragmentation values.

Assuming the projectile has come to thermal equilibrium at an excitation temperature T, Goldhaber[12] has shown that the parabolic shape is again predicted and relates σ_o to T by the equation,

$$kT = 4\sigma_o^2 / M_n B$$

where k is Boltzmann's constant and M_n is the nucleon mass. The measured values of σ_o then reflect excitation energies which can be compared with the nuclear binding energies, Table I. Since the measured excitation energies are nearly equal to the binding energy per nucleon of the projectile, it is inferred that the fragmentation process which results in bound fragments involves very little energy transfer between the target and fragment. The collision is thus very peripheral.

A RECENT NUCLEAR EMULSION EXPERIMENT

^{16}O-Emulsion Nucleus Interactions at 0.15-0.2 and 2 GeV/n

B. Jakobsson, K. Kristiansson, R. Kullberg, B. Lindkvist and I. Otterlund

Abstract of paper to this conference; has observed that the transverse momentum distribution for C, N, and O fragments are Gaussian. Also reactions with three-He fragments are Gaussian. However, if only one or two He nuclei are emitted the deviations from Gaussian are considerable, and the transverse momentum is much larger than predicted by a simple evaporation theory.

FRAGMENTS FROM URANIUM IRRADIATED BY 2.1 GEV/NUCLEON DEUTERONS AND ALPHA PARTICLES

A. M. Zebelman, A. Poskanzer, J. Bowman, R. Sextro, and V. Viola Jr. - Phys. Rev. C. 11 #4 1280 (1975).

Interactions of high energy protons with nuclei are generally described in terms of an intra-nuclear cascade followed by evaporation of one or more mesons and/or nucleons. Except for production of nucleon-antinucleon pairs, the gross features of the reaction are believed to be independent of proton bombarding energy. It appears then that increasing the proton energy above a few GeV does not deposit any more energy in the target nucleus.

This experiment measured the cross section for production of target fragments produced at 90° in the laboratory when protons, deuterons, or α particles were incident on ^{238}U. Fig. 8 shows that, although the cross sections for the production of fragments from Uranium are a factor of 1.5 higher with deuterons than with protons, the energy spectra of these fragments are not significantly different. In contrast, with α particles incident on Uranium there are several indications of increased deposition of energy, and the cross sections are 3 or 4 times greater.

By assuming a Maxwellian evaporation model of the form. $P(\epsilon)=(\epsilon-kB)\ e^{-(\epsilon-kB)/\tau}$ and calculating a classical value for the coulomb barrier, B, the nuclear temperature τ was determined by a best fit to the energy spectrum. The results are given in Table II for incident protons and for α particles.

It is concluded that for α particles compared to protons the effective Coulomb barriers are lower by about 15%, the apparent temperatures are 1.5 MeV higher, the smearing of the energy spectra has increased, and the angular distributions are more forward peaked.

RELATIONS BETWEEN THE CROSS SECTIONS OF VARIOUS PROCESSES AT HIGH ENERGIES.

In 1962 Gribov and Pomeranchuk[14] showed that, to a good approximation, if an interaction can be described by the exchange of a "pomeron" then certain simple relationships are valid for the ratios of total cross sections. The main requirement for this analysis is that the asymptotic behavior of the scattering amplitude of any particles in the diffraction region is determiend by a moving pole j(t) of a particle wave in the annihilation channel.[15] It follows from this assumption that the amplitude of the elastic scattering of strongly interacting particles has the form $f(t)\ S^{j(t)}$, where s and t are the standard Mandelstam variables. The total cross section is constant if $j(o)=1$ the maximum value. The elastic cross section approaches zero as $[\ln s]^{-1}$ and the diffraction cone narrows with increasing energy. Thus, the scattering system is more transparent and the radius of the interaction increases with energy. This behavior has been observed for PP and πP systems with the ex-

ception of very high energies, 200 GeV and greater, where the cross sections again increase. It is reasonable to expect this behavior for all hadron-hadron system, i.e. for systems with baryon number $B \geq 1$.

The closely related concepts of scaling and factorization are valid for nuclear systems at high energy. The high energy heavy ion production and scattering experiments should then provide an extremely powerful means of studying nuclear correlations inside nuclei. Allowing the baryon number to increase introduces an additional degree of freedom, and places additional constraints on models of high energy collisions.

The factorizability of total cross section σ_{AB} is related to the cross section σ_{AA} and σ_{BB} by

$$(\sigma_{AB})^2 = \sigma_{AA}\ \sigma_{BB}$$

As a simple example, consider nucleus A incident on nucleus A

Then, $\sigma_{AA} = \frac{(\sigma_{PA})^2}{\sigma_{PP}}$

where σ_{PP} is the total proton-proton cross section.

Since $\sigma_{PA} \propto A^{2/3}$, this relation leads to the prediction

$$\sigma_{AA} \propto A^{4/3}$$

Gribov[16] pointed out that this is possible at high energies if the nucleus becomes larger and at the same time more transparent. However, this is an unlikely behavior and various geometric models predict an $A^{2/3}$ dependence for Nucleus-Nucleus total cross sections. Fishbane and Trefil[17] and Barshay et. al.[18] have predicted that factorization holds to 20% if the radii of the target and projectile nuclei do not differ by more than 50%.

In a recent experiment,

MEASUREMENT OF TOTAL NUCLEUS-NUCLEUS CROSS SECTIONS,
at 0.87 and 2.1 GeV/nucleon.
(J. Jaros, L. Anderson, O. Chamberlain, R. Fuzesy,
J. Gallup, W. Corn, L. Schroeder, S. Shannon, G. Shapiro,
H. Steiner, A. Wagner, J. Wises, LBL and John Jaros
LBL 3849 (Thesis).

A systematic study was made to determine σ_T for all target-projectile combinations of P, d, ^{4}He, and ^{12}C at 0.87 and 2.1 GeV/n. The goal was to test the validity of the factorization relation,

σ_{AA} $\sigma_{BB} = \sigma^2_{AB}$ for total cross sections. The separation of the nuclear and coulomb effects are major theoretical and experimental problems. In addition to σ_t, the values of σ_{in} and the elastic slope parameter b have been measured. The data are in good agreement with Glauber type calculations at 2.1 GeV/n. The naive factorization predictions for σ_t(CC) differ by a factor of two. Also, the total cross section σ_t(Pα), σ_t(PC), and α_t(CA) where (A=P,d, α, c) all show substantially greater percentage variations between 0.87 and 2.1 GeV/n than do σ_t(PP) and σ_t (P,n).

A plot of the preliminary data is given Fig. 9, and the energy dependence of σ_t is shown in Fig. 10. Also, recent measurements have been made,

PROJECTILE FRAGMENTATION AND PION PRODUCTION BY LIGHT RELATIVISTIC IONS ON NUCLEI.

(James Papp, J. Jaros, L. Schroeder, H. Steiner, J. Staples, A. Wagner and J. Wiss, LBL and James Papp LBL 3633 (Thesis).

The pion results will be presented in another paper at this conference.

The fragments produced by p, d, α, and C on Targets of Be, C, Cu, and Pb were detected at 2.5^0 lab. The single particle inclusive spectra, Fig. 11, P, d, ^{3}H and ^{3}He produced by 1.05 GeV/n α particles on Be show peaks associated with projectile fragmentation, plus central collision plateaus. In this frame it is observed that the heavier the fragment, the narrower the projectile fragment peak. A direct comparison between the single particle proton spectra as a function of rapidity for 2.1 GeV/n deuterons and alphas on Be is given, Fig.12. The proton distribution from the deuterons is narrower than from alphas, showing that the momentum distribution of protons in deuterons is not as broad as that in alpha particles.

For production of particles with baryon number B $\geq$1 the data are consistent with limiting fragmentation of the projectile. Since the data are for fixed lab angle rather than for fixed transverse momentum a decisive test of limiting fragmentation was not made. However, the method can be extended and become an excellent method to study correlations inside nuclei.

Other fascinating fragmentation processes are:

1) Nuclear shock waves
2) Production of Ultradense matter.

For some collisions of relativistic heavy ions with a high Z target, low relative momentum between the ions and target could produce compressed nuclear matter[19]. This might be detected as nuclear shock waves.

Some experiments have been done to investigate these phenomena;

SEARCH FOR NUCLEAR SHOCK WAVES IN HIGH ENERGY NUCLEUS-NUCLEAR COLLISIONS.

B. Schopper, H. G. Baumgardt, J. U. Schoot, Y. Sakamoto
Preprint 1975.

ABSTRACT: Nucleus-Nucleus collisions are produced in track-detectors, monocrystalline layers of AgCl, by monoenergetic ions of oxygen at 2.1; 0.8751 0.25 GeV/N. Angular distributions of the particles and fragments from star-events at the Ag and Cl nuclei of the detector are studied in 4π geometry. Peaks in the angular distribution at forward and backward angles shifting with the projectile energy, as well as clustering effects, suggest their interpretation as signatures for shock waves.

And,

VERY ENERGETIC HEAVY FRAGMENTS FROM RELATIVISTIC HEAVY-ION REACTIONS

H. H. Crawford, P. B Price, J. Stevenson, and Lance W. Wilson
Phys. Rev. Lett, 34, 329 (1975).

ABSTRACT: In bombardments of Au with 25-GeV ^{12}C ions we have studied the energy and angular distribution of fragments with $5 \leq Z \leq 9$ emitted at energies up to ∿ 1000 MeV. Beyond ∿150 MeV the spectra change from roughly exponential in energy and isotropic in some forward-moving frame to roughly inverse power law in energy (steepening with increasing Z) and strongly forward peaked in direction. Possible bumps in the angular and energy distributions suggest hydrodynamic effects.

ULTRADENSE NUCLEI

Abnormal dense matter might be produced by high energy heavy ion collisions[20-24]. In this case the extra energy of compression is assumed to be transformed to a massive meson resonant state. Lee[22] has considered a specific model of a scalar meson field coupled to a nucleon field of strength such that the effective mass of each nucleon is reduced to zero near the Fermi surface. Under these conditions, the binding energy of the nucleon is increased from 16 MeV/nucleon to about 160 MeV/nucleon.

Thus stable heavy nuclei are predicted.

The highest mass relativistic heavy ion that has been available is Ar. A "preliminary experiment" has been done.

SEARCH FOR ULTRADENSE NUCLEI IN RELATIVISTIC COLLISIONS OF AR ON PB.

P. B. Price and J. Stevenson
Phys. Rev. Lett. 34 No. 7, 409 (1975)

Abstract: In 2.5×10^8 interactions of 1.1- to 1.6 -GeV/Nucleon ^{40}Ar ions with a Pb target we saw no tracks of products with Z >20 ejected in the beam direction, using a Lexan detector stack. The upper limit on the formation cross section is about 50 nb for products with $26 \leq Z \leq 40$ and increases with Z to about 1.5μb for Z=100.

In conclusion, if a new ultra-dense state of matter can be shown to exist, then the entire system of meson physics will have to fit into a new pattern!

Table I. Comparison with theory and experiment of parameters related to a $\sigma_{P_\parallel}$ mass dependence of the form $\sigma_{P_\parallel}^2 = 4\sigma_o^2 F(B-F)/B^2$. Derived quantities are Fermi momentum $P_f = 2\sigma_o^2(B-1)/B^2$ and average excitation energy $kT = 4\sigma_o^2/m_n B$.

Parameter	Origin	Projectile		
		^{16}O 2.1 GeV/n	^{12}C 2.1 GeV/n	^{12}C 1.05 GeV/n
σ_o(MeV/c)	this expt.	171±3	147±4	141±5
"	sudden approximation[7]	162	145	145
"	virtual clusters[8]	212	179	179
P_f(MeV/c)	this expt.	185±3	182±5	174±6
"	electron scattering[10]	230	221	221
kT(MeV/n)	this expt.	7.8±0.3	7.7±0.4	7.1±0.5
average binding energy (MeV/n)	mass measurements	8.0	7.7	7.7

TABLE II. Parameters obtained in the curve fitting.

Isotope	B (MeV)	Incident Protons					Incident Alphas				
		$< k > \pm \Delta$	90^{o} peak energy (MeV)	τ (MeV)	τ_T^* (MeV)	$< v >/c^{\dagger}$	$< k > \pm \Delta$	90^{o} peak energy (MeV)	τ (MeV)	τ_T^* (MeV)	$< v >/c$ (MeV)
^{4}He	22	0.58 ± .2	20	6	19	0.003	0.48 ± .3	20	6.5	16	< 0.01
^{6}He	22	0.60 ± .1	24	9	16		0.50 ± .3	23	10	18	<0.01
^{6}Li	32	0.57 ± .1	32	13	18	0.006	0.52 ± .2	33	13.5	19	<0.01
^{7}Li	32	0.58 ± .25	31	10	15	0.005	0.48 ± .38	30	12	19	<0.02
^{7}Be	42	0.54 ± .25	41	17	19	0.007	0.48 ± .35	37	19	22	<0.01
^{9}Be	41	0.58 ± .05	36	12	13	0.007	0.48 ± .15	35	13.5	19	<0.03
^{10}Be	41	0.58 ± .05	36	12	15	0.007	0.52 ± .15	35	13.5	17	<0.01
^{11}Be	50			13		0.006			15		<0.01

*τ_T refers to the temperature needed to fit the high energy tail of the spectrum.

† Data from Reference 6.

REFERENCES

1. G. F. Chew, LBL - Heavy Ion Summer Study 1973.
2. G. F. Chew, Comments on Nuclear and Particle Physics II, 107, 1968.
3. R. Silberberg and C. H. TSAO NRL Report 7593 (1973).
4. F. Yiou, G. Raisbeck, C. Perron, and P. Fontes, Conference Papers, 137H International Cosmic Ray Conf. Denver Colorado 17-30 Aug. 1973, Vol. 1, Paper # 251.
5. H. H. Heckman and P. J. Lindstrom - To be published.
6. R. Hofstadter and H. R. Collard - Nuclear Radii determined by electronic scattering P21, Landolt-Bornstein, New Series I/2 Springer-Verlag (1967),
7. D. E. Greiner, P. J. Lindstrom, H. H. Heckman, Bruce Cork, and F. S. Bieser LBL Report 3651 (1975) To be published.
8. W. R. Fraser et. al., Rev. Mod. Phys. 44, 284 (1972).
9. W. A. Wenzel, LBL Heavy Ion Seminar (1973 unpublished).
10. J. V. Lepore and R. J. Riddell Jr., LBL 3086 (1974) (unpublished).
11. H. Feshbach and K. Huang. Phys. Lett. 47B, 300 (1973).
12. A. S. Goldhaber Phys. Lett. 53B, 306 (1974).
13. V. K. Lukyanov and A. I. Titov. To be published and Contribution to this conference.
14. V. N. Gribov and I. Ya. Pomeranchuk, Phys. Rev. Lett. 8 #8, P343 (1962).
15. G. F. Chew and S. Frautschi, Phys. Rev. Lett. 7, 394 (1961).
16. V. N. Gribov, Soviet Journal of Nuclear Physics, 9, 369, (1969).
17. P. M. Fishbane & J. S. Trefil Phys. Rev. Lett. 32, 396 (1974).
18. Saul Barshay, C. B. Dover, and J. P. Vary. Phys. Rev. C. 11, 360, (1975).
19. For a review, see W. Greiner and W. Scheid, J. De PHYSIQUE 32 (1971) C6-91 and Proceedings, 2nd High Energy Heavy Ion Summer Study July 15-26, 1974 at Lawrence Berkely Lab. LBL 3675.
20. A. R. Bodmer, Physl Rev. D 4 1601 (1971).
21. A. B. Migdal, Zh. Eksp. Teor. Fiz 61, 2209 (1971). (Sov. Phys. JETP 34, 1184 (1972)).
22. T. D. Lee and G. C. Wick, Phys. Rev. D 9, 2291, (1974).
23. G. F. Chapline, M. H. Johnson, E. Teller, and M. S. Weiss, Phys. Rev. D. 8 4302 (1973).
24. L. CastilleJo paper at this conference.

This work was performed under the auspices of the U.S. Energy Research and Development Administration and the National Aeronautics and Space Administration Grant NGR 05-003-513.

FIGURE CAPTIONS

1. Three different fragmentation processes.
2. Emulsion photograph of fragmentation of Ar projectile.
3. Emulsion photograph of fragmentation of the target.
4. The cross sections for B+T → F + — can be expressed as $\sigma_{BT}^{F} = \gamma_{B}^{F} \gamma_{T}$ where γ_T is the target factor. The line superimposed on the data points is an approximation for $\gamma_T = A_T^{\frac{1}{4}}$
5. Photo production of giant dipole resonance. Deviation of target factor γ_T from average target factor as a function of atomic weight A_T
6. The projectile-frame parallel—momentum distribution for ^{10}Be fragments from ^{12}C at 2.1 GeV/N on a Be target. The curve is a best fit to a Gaussian momentum distribution.
7. Plotted are the target-averaged width $\sigma_{P_\parallel}$ of the projectile-frame parallel-momentum distribution in MeV/cversus fragment mass in AMU.
8. Ratios of Energy Spectra at 90^{o} in the laboratory for a) incident deuterons to incident protons, and b-c) for incident alphas to incident protons.
9. Jaros. Total cross section vs atomic number A for 2.1 GeV/n projectiles.
10. Jaros. Energy dependence of total cross sections for protons and for carbon projectiles.
11. Invariant cross section as a function of fragments produced by 1.05 GeV/n alpha particles on Be.
12. Comparison of the single particle inclusive proton rapidity distributions resulting from the fragmentation of 2.1 GeV/n deuterons and alphas on a Be target.

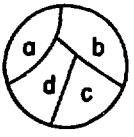

X=-1

TARGET FRAGMENTS

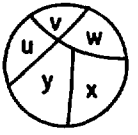

X=0

PIONIZATION REGION (BOTH)

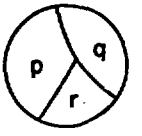

X=+1

PROJECTILE FRAGMENTS

$$X \simeq \frac{E^{C}(LAB)}{E_{TOT}(LAB)}$$

XBL 755-1368

Fig. 1

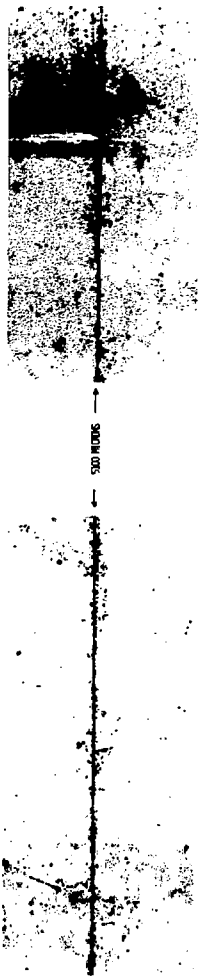

XBB 7411-8294

Fig. 2

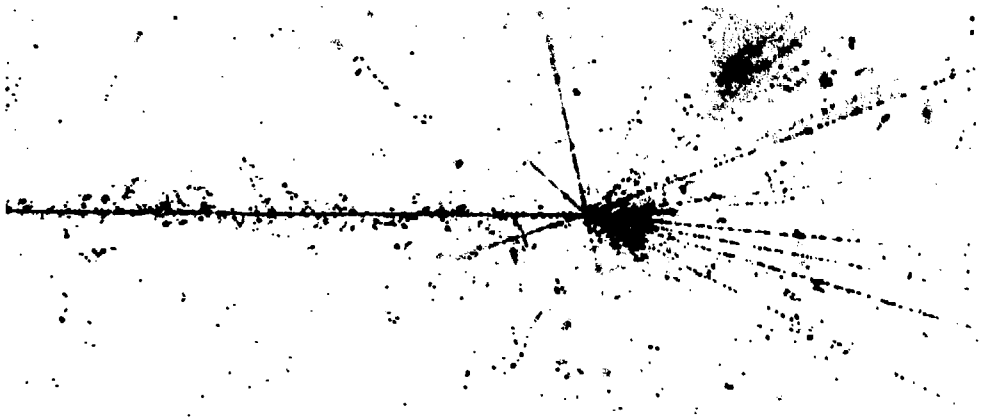

XBB 7411-8295

100 MICRONS

Fig. 3

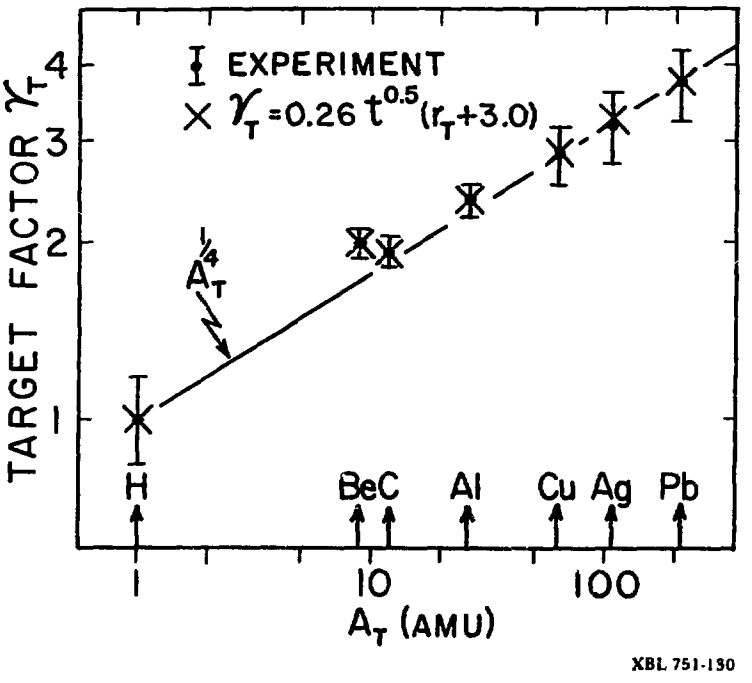
EXPERIMENT
$\gamma_T = 0.26\, t^{0.5}(r_T+3.0)$
$A_T^{1/4}$
TARGET FACTOR γ_T
1
2
3
4
H
BeC
Al
Cu
Ag
Pb
1
10
100
A_T (AMU)
XBL 751-130

Fig. 4

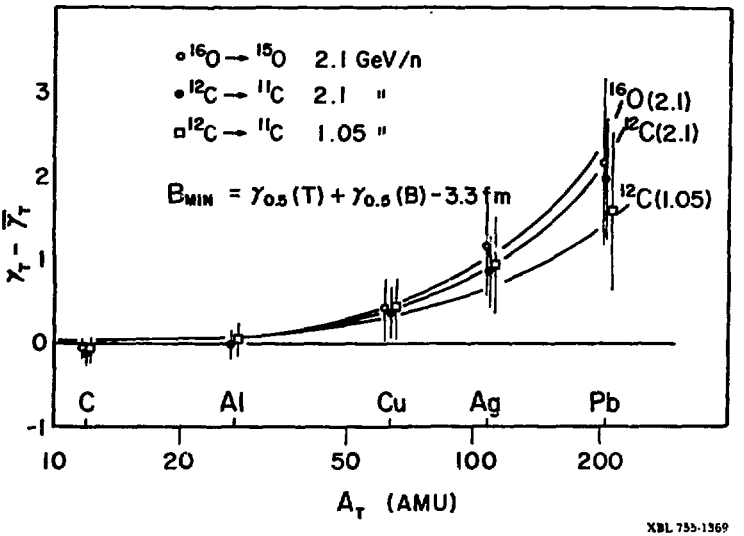
$\circ\ ^{16}O \rightarrow\ ^{15}O$ 2.1 GeV/n
$\bullet\ ^{12}C \rightarrow\ ^{11}C$ 2.1 "
$\square\ ^{12}C \rightarrow\ ^{11}C$ 1.05 "
$B_{MIN} = \gamma_{0.5}(T) + \gamma_{0.5}(B) - 3.3$ fm
$^{16}O(2.1)$
$^{12}C(2.1)$
$^{12}C(1.05)$
$\chi_T - \overline{\chi}_T$
3
2
1
0
-1
C
Al
Cu
Ag
Pb
10
20
50
100
200
A_T (AMU)
XBL 755-1369

Fig. 5

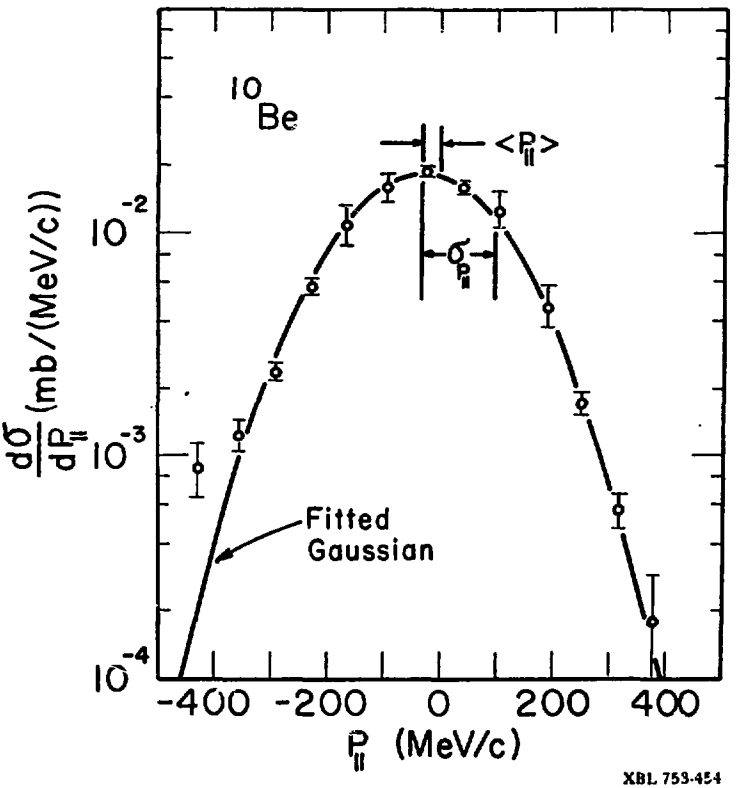
^{10}Be
$\langle P_{\parallel} \rangle$
$\sigma_{P_{\parallel}}$
Fitted
Gaussian
$\frac{d\sigma}{dP_{\parallel}}$ (mb/(MeV/c))
10^{-2}
10^{-3}
10^{-4}
-400
-200
0
200
400
$P_{\parallel}$ (MeV/c)
XBL 753-454

Fig. 6

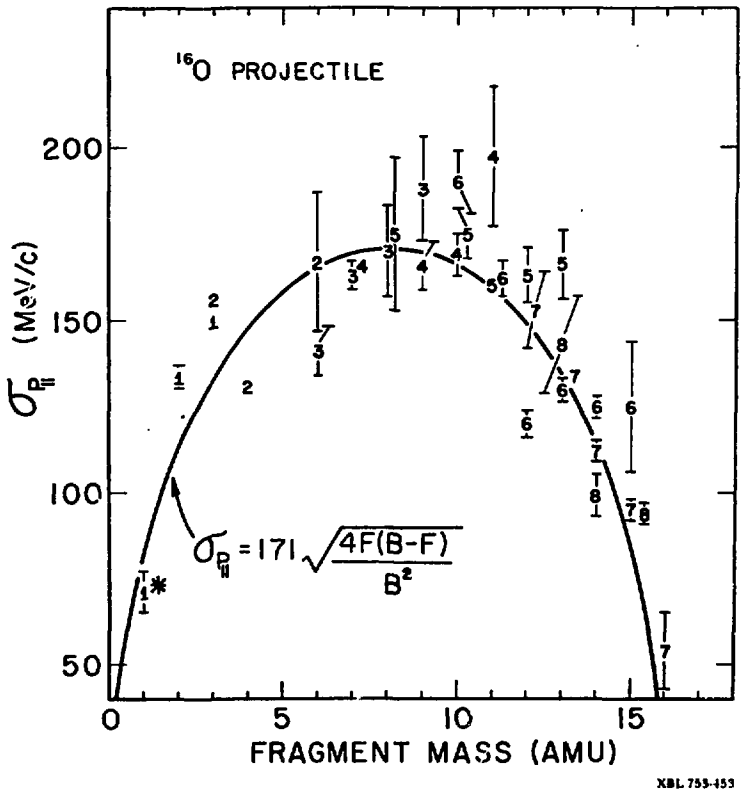
^{16}O PROJECTILE
200
150
100
50
$\sigma_{p_{\parallel}}$ (MeV/c)
0
5
10
15
FRAGMENT MASS (AMU)
$\sigma_{p_{\parallel}} = 171\sqrt{\frac{4F(B-F)}{B^2}}$
XBL 755-453

Fig. 7

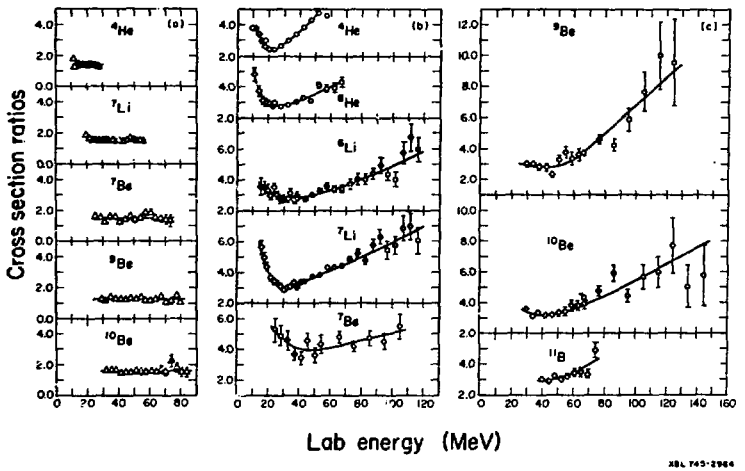
Cross section ratios
Lab energy (MeV)
(a)
(b)
(c)
4He
7Li
7Be
9Be
10Be
6He
6Li
11B

Fig. 8

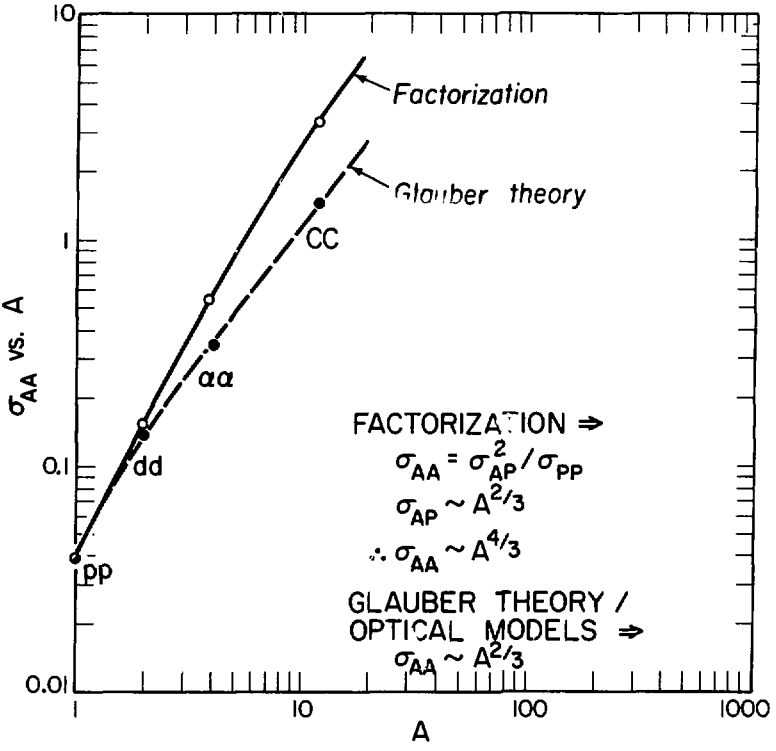
10
1
0.1
0.01
σ_{AA} vs. A
Factorization
Glauber theory
CC
αα
dd
pp
FACTORIZATION ⇒
$\sigma_{AA} = \sigma_{AP}^2 / \sigma_{PP}$
$\sigma_{AP} \sim A^{2/3}$
$\therefore \sigma_{AA} \sim A^{4/3}$
GLAUBER THEORY /
OPTICAL MODELS ⇒
$\sigma_{AA} \sim A^{2/3}$
1
10
100
1000
A
XBL 756-3123

Fig. 9

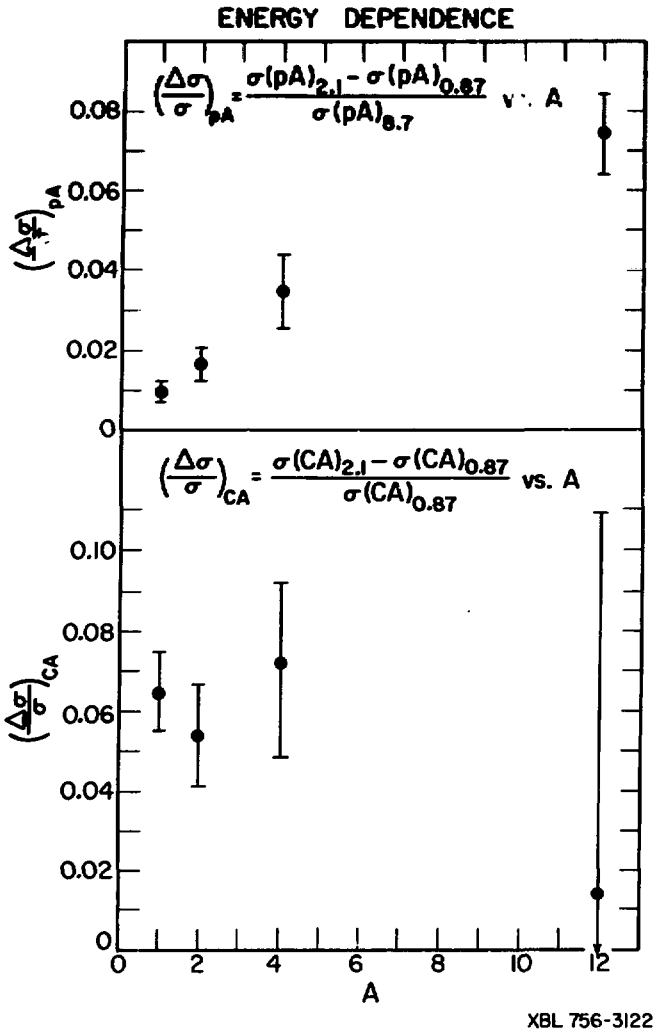
ENERGY DEPENDENCE
$\left(\frac{\Delta\sigma}{\sigma}\right)_{pA} = \frac{\sigma(pA)_{2.1} - \sigma(pA)_{0.87}}{\sigma(pA)_{8.7}}$ vs. A
$\left(\frac{\Delta\sigma}{\sigma}\right)_{pA}$
0.08
0.06
0.04
0.02
0
$\left(\frac{\Delta\sigma}{\sigma}\right)_{CA} = \frac{\sigma(CA)_{2.1} - \sigma(CA)_{0.87}}{\sigma(CA)_{0.87}}$ vs. A
$\left(\frac{\Delta\sigma}{\sigma}\right)_{CA}$
0.10
0.08
0.06
0.04
0.02
0
0
2
4
6
8
10
12
A
XBL 756-3122

Fig. 10

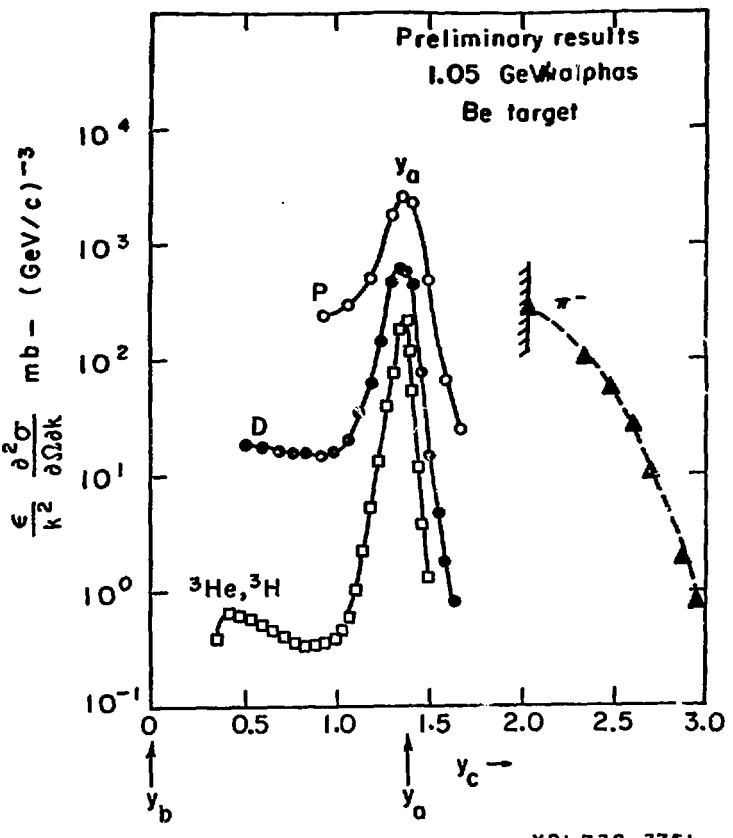
Preliminary results
1.05 GeV/c alphas
Be target
$\frac{\epsilon}{k^2}\frac{\partial^2\sigma}{\partial\Omega\partial k}$ mb – (GeV/c)$^{-3}$
10^4
10^3
10^2
10^1
10^0
10^{-1}
y_a
P
D
^{3}He,^{3}H
π^-
0
0.5
1.0
1.5
2.0
2.5
3.0
y_c →
y_b
y_a
XBL738-3751

Fig. 11

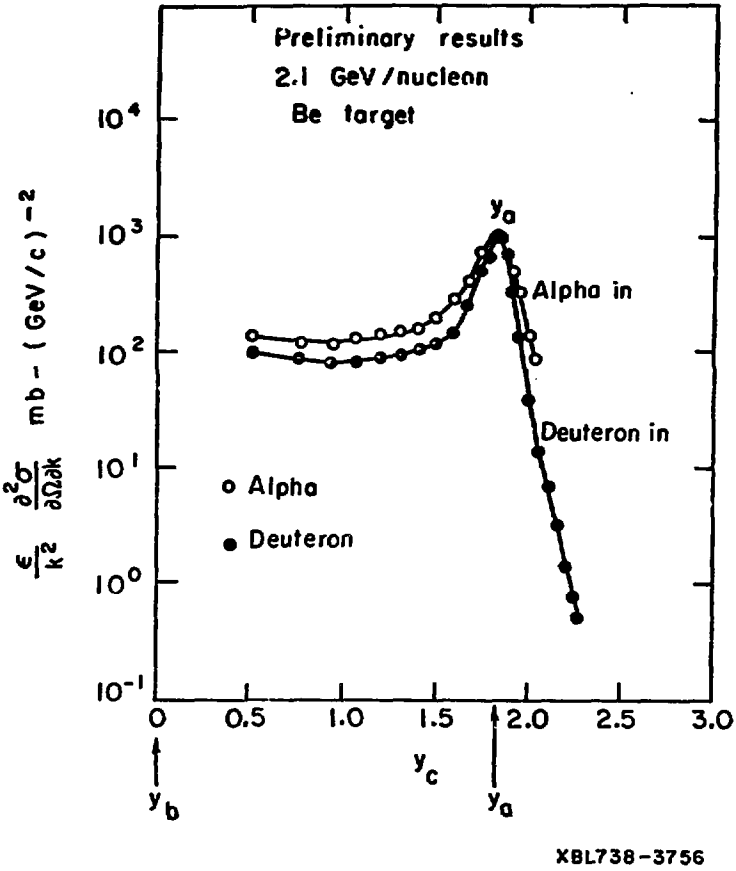
Preliminary results
2.1 GeV/nucleon
Be target
$\frac{\epsilon}{k^2}\frac{\partial^2\sigma}{\partial\Omega\partial k}$ mb - (GeV/c)$^{-2}$
10^4
10^3
10^2
10^1
10^0
10^{-1}
y_a
Alpha in
Deuteron in
o Alpha
● Deuteron
0
0.5
1.0
1.5
2.0
2.5
3.0
y_b
y_c
y_a
XBL738-3756

Fig. 12